Effects of Fusion Zone Size on Failure Modes and Mechanical Performance of Dual Phase (DP600) Steel Sheets Spot Welds.

Fadhel A. Hashim[1], Raid K. Salim[2] and Hassanen L. Jaber[3]
1: University of Technology 2: Technical College – Baghdad
3: University of Thi-Qar/ Engineering College/ Mechanical department(hasnen1983@gmail.com)

الخلاصة

يهدف البحث الى دراسة تأثير حجم منطقة اللحام والتركيب المجهري للوصلات الناتجة من لحام المقاومة النقطي لفولاذ ثنائي الطور و شكل الفشل لهذه الوصلات، تم استخدام المجهر الالكتروني الماسح في دراسة التراكيب المجهرية في حين استخدام اختبار الشد-القص لدراسة الخواص الميكانيكية و تحديد نوع او شكل الفشل.

بينت النتائج ان التركيب المجهري لمنطقة الانصهار عباره عن مارتنسايت بقيمة صلاده قدرها ٤٥٠ فيكرز، اما المنطقة المتأثرة بالحرارة فهي عبارة عن فوق الحرجة و تركيبها مارتنسايت صلادته ٤٢٠ فيكرز والمنطقة ما بين الحرجة بتركيب مارتنسايتي-فرايتي لتنخفض صلادتها الى ٣١٠ فيكرز، كذلك بينت النتائج ان نوع (شكل) الفشل يعتمد على مقدار التيار المستخدم حيث ان الفشل يتحول من بيني الى انجراري (انسحابي) عند قيمة تيار قدرها ٨،٥.

ABSTRACT

This paper examines the effects of fusion zone size on failure modes, quasi tension -shear test and energy absorption of resistance spot welds (RSW) of dual phase (DP600) steels. Optical microscopy was used for microstructure investigation. The results showed that some samples failed in pullout failure mode and other samples failed in interfacial failure mode and the failure was located at the base metal. The conventional weld size guidance of $4t^{0.5}$ and $5t^{0.5}$is not sufficient to produce nugget pullout failure mode for DP600 resistance spot welds.

KEYWORDS: Dual-Phase Steels, Shear-Tension Test, Failure Mode and Resistance Spot Weld

INTRODUCTION

Advanced high-strength steels (AHSSs) have been used in the automotive industry as a solution for the weight reduction, safety performance improvement and cost saving[1- 4]. The Ultra-Light Steel Auto Body (ULSAB) project has shown that

car body mass can be reduced by 25% using advanced high-strength steels (AHSS) and innovative processes[5,6]. It is anticipated that AHSS usage in automotive bodies will climb to 50% by 2015[7].

Dual phase (DP) steels are one of the most common AHSS steels. Dual phase (DP) steels possess a unique microstructure consisting of soft ferrite and hard martensite that offers favorable combination of strength, high work-hardening rate, ductility and formability [2,8]. DP steels are commercially available at present in 500, 600, 780, and 980 MPa minimum tensile strength levels. In recent years, DP600 applications are widely used in different automobile models such as Porsche Cayenne, Land Rover LR2 and Jaguar XF fig. (1)[3,9]. Compared to High-strength low-alloy (HSLA) steels, DP600 steels exhibit a slightly lower yield strength, a continuous yield behavior due to enough active slip systems in the ferrite phase, and a more uniform and higher total elongation (over 21%)[5,7,8].

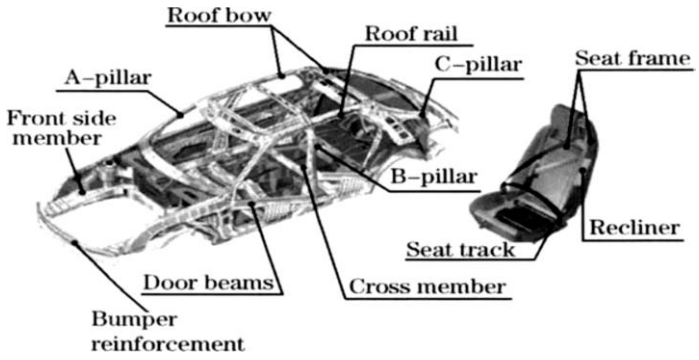

Fig. (1): The automobile parts in which DP 600 steel is used **[**3**].**

DP steels are joined by several welding methods. Resistance spot welding (RSW) is the main joint method of assembly auto body due to its high efficiency in processing thin DP steel sheets. RSW for DP steels is the simplest, fastest, and most controllable. Hence, the automotive industry uses RSW at several thousand welding points about (2000–5000) spot welds in each automotive body structures[10,11]. Therefore, there is a need to study the spot welding behavior of this materials. Generally, there are three measures for quality evaluation of resistance spot welds including physical weld attributes (e.g. fusion zone size,), mechanical properties and failure mode[12,13].

1-1 Physical and metallurgical weld attributes

1 - weld nugget or FZ size (d) which is defined as the width of the weld nugget at the sheet/sheet interface in the longitudinal direction (Fig(2)) is the most important factor in determining the quality of spot welds. Quantitative measurements of the weld size were conducted in two ways: (i) from the weld button diameter on test coupons with a digital calliper (ii) from the cross-section of weld nugget[12,14].

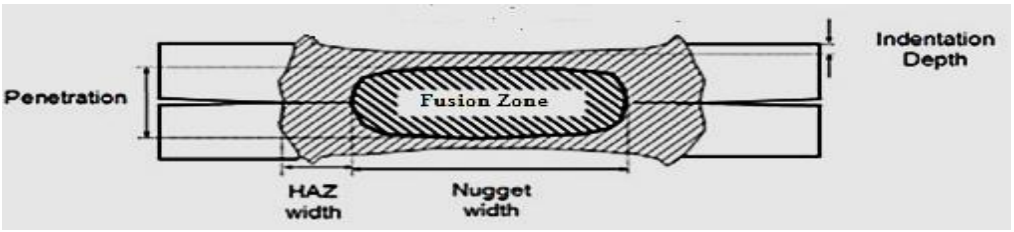

Fig (2) : Geometric Attributes of the Spot Weld [15]

2 – *Expulsion*: The expulsion is The ejection of molten metal from the faying interface (interface between two test coupons) of the samples and observing whether metal "whiskers" or "fingers" are evident at the interface and can lead to a lack of material to fill the weld nugget upon solidification Fig (3).[12,13]

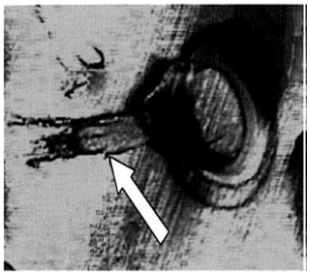

Fig (3) : Expulsion traces at the faying interface of a steel weld [13].

3- *hardness and material properties of fusion zone(*FZ) *and heat affected zone (*HAZ): Hardness and material properties of FZ and HAZ are controlled by the interaction of weld thermal cycle, chemical composition and the initial microstructure of the base metal[16].

1-2 Failure mode

Failure mode of resistance spot welds is a qualitative measure of mechanical properties[13]. Basically, spot welds can fail in two distinct modes described as follows:(i) Interfacial mode (IF), In the IF mode, failure occurs via crack propagation through fusion zone, often occurring in a small weld. The weld fails at the interface of the two sheets, leaving half of the weld nugget in one sheet and half in the other sheet Fig(4) [17].

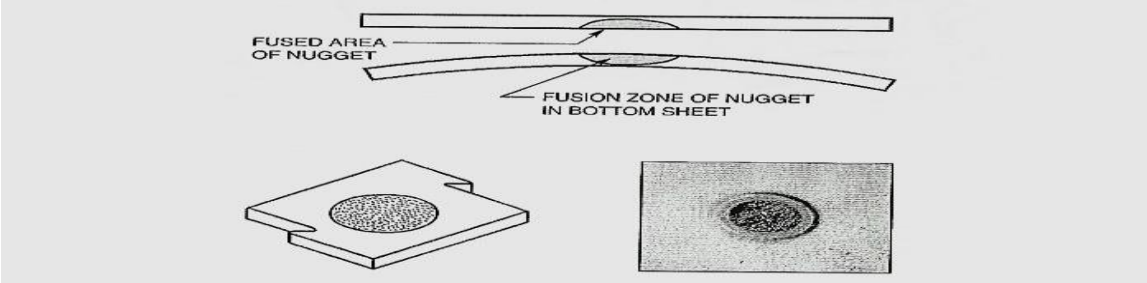

Figure (4): Interfacial Fracture [12]

(ii) pullout failure (PF) occurs via nugget withdrawal from one of the sheets, the weld nugget is completely pulled out from one of the metal sheets, leaving a circular hole in the sheet Fig (5). Some of them failed via complete nugget pullout failure from two sheets called (double pullout) (DPF) while, others experienced sheet tearing after nugget withdrawing from one sheet [17]. Generally, the PF mode exhibits the most satisfactory mechanical properties. Therefore, it is needed to adjust welding parameters so that the PF mode is guaranteed.

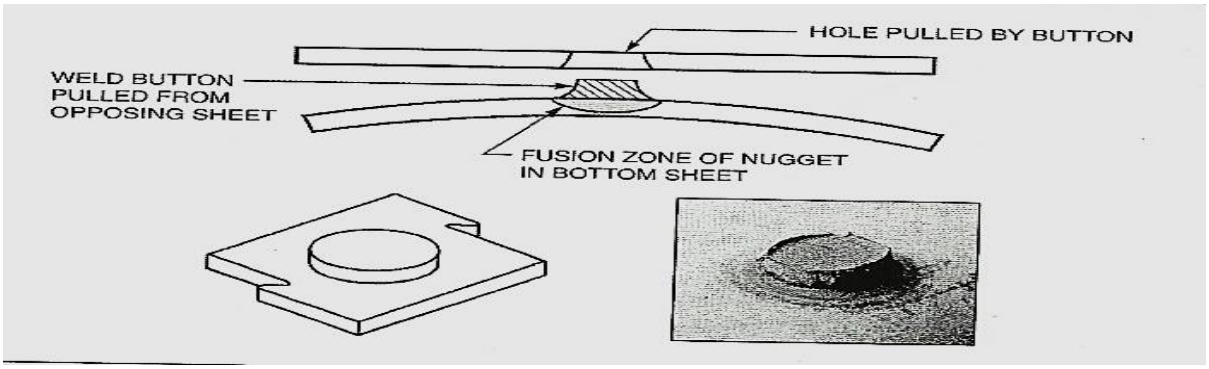

Figure (5) : (a) Button Pull Fracture[12]

1-3 Failure mode prediction

Various industrial standards have recommended a minimum weld size for a given sheet thickness, in order to ensure the PF mode as shown in fig (6).

1 - According to AWS/ANSI/AISI [12], weld button sizing to ensure that the weld size was large enough to carry the desired load, is based on the Equation (1)

$$dc = 4t^{0.5} \quad (1)$$

where, dc is critical fusion zone size in mm, t is sheet thickness in mm.

2 - According to Japanese JIS Z3140[18] and the German DVS 2923[19] standards, the required weld size is specified according to equation (2).

$$dc = 5t^{0.5} \quad (2)$$

3 - Pouranvari and Marashi[16,20] based on the failure mechanism of the spot welds in the tension shear test, proposed a simple analytical model to predict the minimum FZ size (d_c) to ensure the PF mode as shown in equation (3).

$$d_c = \frac{4t}{pF}\left(\frac{HPFL}{HFZ}\right) \quad (3)$$

where t is the sheet thickness (mm), P is the porosity factor and its value (0-1), F = (0.5) is the ratio of shear strength to tensile strength of the F_Z, H_{FZ} and H_{PFL} are hardness values (HV) of the FZ and PF location respectively.

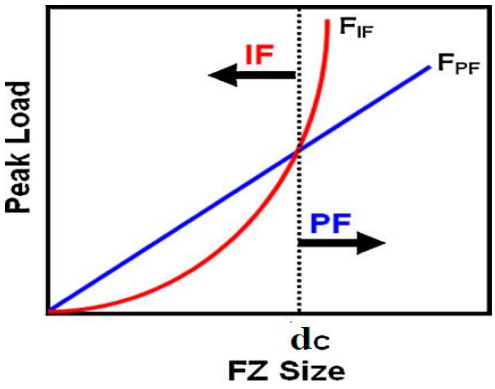

Fig (6): plot of peak load versus fusion zone size both interfacial and pullout failure modes [16]

2 - Experimental procedure

A 1.5 mm thick DP600 dual phased steel sheets were used as the base metals. The chemical composition of the base metals is presented in Table 1. The mechanical properties of the base metals were determined using a standard tensile test in accordance to ASTM E8. Fig. 7 shows the mechanical properties of the investigated steels.

Table (1) Chemical composition of DP600 steel

Element % / Steel		C	Mn	P	S	Si	Cr	Mo	V	Nb	Cu	Ni	Fe
DP600	Actual	0.07	1.52	0.008	0.011	0.048	0.1	0.02	0.01	0.005	0.03	-	Base
	Nominal	0.06-0.15	1.5-2.5	-	-	-	0.4	0.4	0.06	0.04	-	-	-

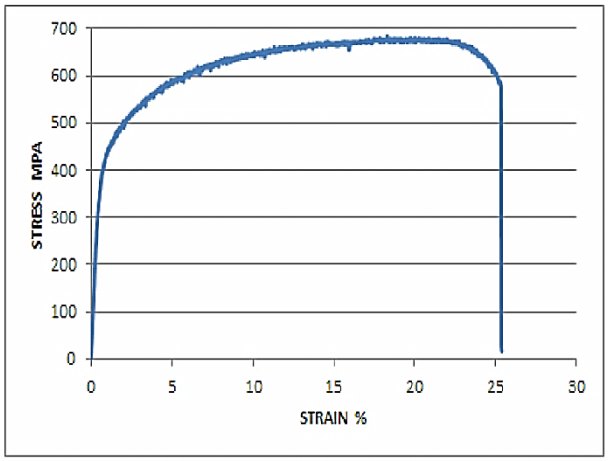

Figure (7) stress vs. strain curves for DP600.

Welding process was performed by a 120 kVA ac pedestal type resistance spot welding machine, controlled by a programmable logic controller. Welding was conducted using a 90° truncated cone Resistance Welding Manufacture Association RWMA Class two electrodes[12], with face diameter of 6 mm. The welding process was carried out with a constant electrode pressure of 4 bar. Squeeze time, welding time and holding time were kept constant at 45, 15 and 10 cycles, respectively. Experiments were done with changing the welding current from 6 to 13 kA.

The samples for the tensile-shear test were prepared according to ANSI/AWS/SAE/ D8.9-2012 standard[12] fig. (8). The tensile shear test was performed by an Instron universal testing machine at a cross head of 2 mm/min. Standard metallography procedure was conducted to examine the microstructure of fusion zone and heat affected zone by optical microscopy . The fusion zone size was measured on the metallographic cross sections and digital calliper. Vickers micro-hardness test was performed to obtain hardness profile using an indenter load of 200g.

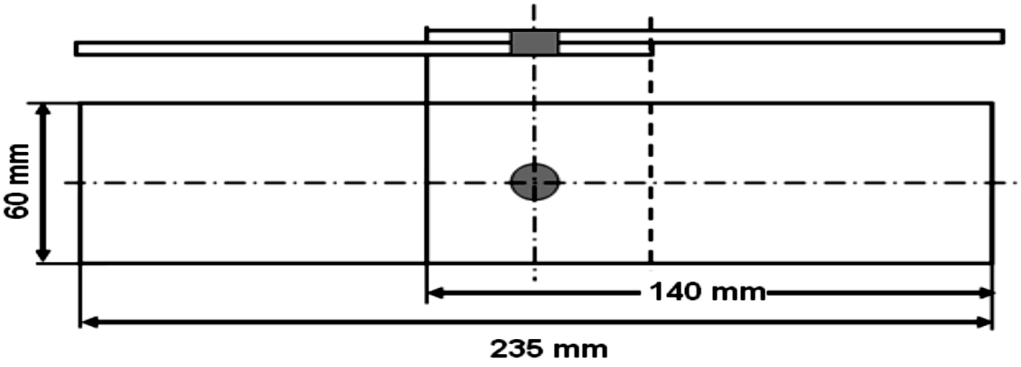

Figure (8):Test configuration and sample dimensions of tensile shear test

Peak load (measured as the peak point in the load–displacement curve) and the failure energy (measured as the area under the load–displacement curve up to the peak load)[13]fig. (9) were extracted from the load–displacement curve by using the concept of Riemann Sums equation (4). The data points for peak load and failure energy are averages of the measured values for the three specimens.

$$\int_0^{Lmax} \mathbf{Fdx} = \sum_{n=1}^{N} \mathbf{F(n).[L(n) - L(n-1)]} \qquad \mathbf{(4)}$$

where F is the load, X the displacement, L_{max} the displacement at the peak load, n the sampled data and N the peak load.

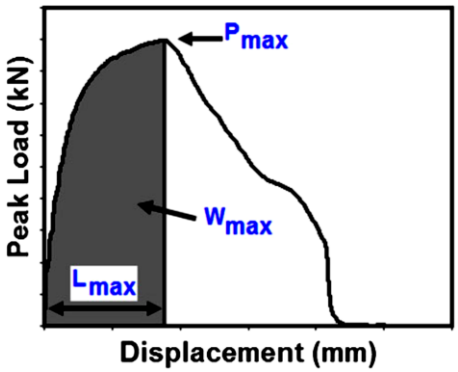

Fig. 9. Load–displacement curve of spot welds during tensile-shear test[13].

3- Results and discussions

3-1 Effect of Welding Current on Weld physical Attributes

Fig. (10a) shows the effect of welding current on the peak load of welds indicating that generally increasing welding current increases the load bearing capacity. However, at high heat input welding condition (welding current beyond 11kA), peak load is reduced due to expulsion. Fig. (10b) shows the effect of welding current on the failure energy indicating that increasing heat input caused by increasing welding current increases the energy absorption capability of the welds. However, at high heat input welding condition (welding current beyond 11kA) energy absorption is significantly reduced due to expulsion as shown in fig. (11).

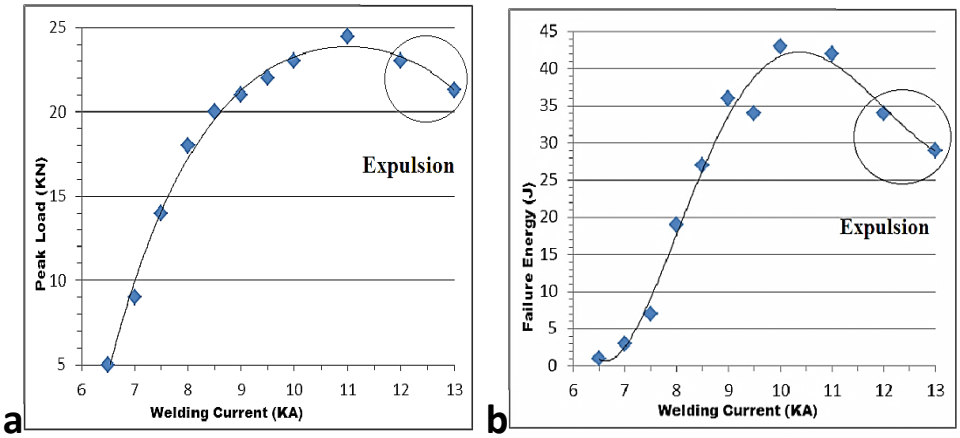

Fig (10): (a): Effect of welding current on the peak load, (b) Effect of welding current on the failure energy.

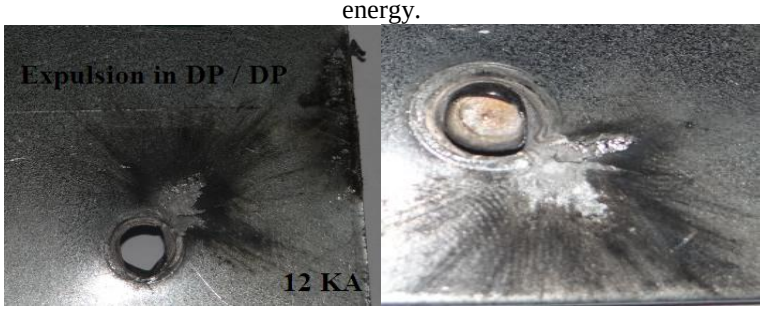

Fig (11): Expulsion traces at the faying interface of DP/DP RSW.

Fig. (12a) shows the effect of FZ size on the peak load. As can be seen, there is a direct correlation between FZ size and peak load. Fig. (12b) shows the effect of FZ size on the failure energy indicating that there is a direct correlation between FZ size and the failure energy.

According to fig. (12a, b), fusion zone size is the most important controlling parameter of peak load and energy absorption of the DP600 spot welds. Similar conclusion was obtained for galvanized low carbon steel [21], TRIP800 steel, DP800 [1]. In summary, increasing welding current results in higher heat generation at the faying interface resulting in the formation of larger fusion zone and increases overall bond area. These facts can explain increasing in peak load and energy absorption until optimal welding conditions are received.

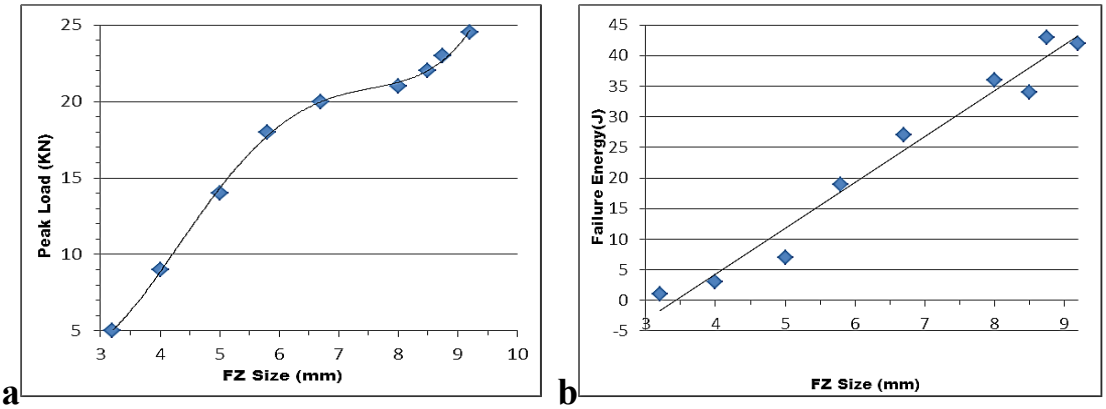

a b

Fig (12):**(a)**: Effect of fusion zone size on the peak load , **(b)**: Effect of fusion zone size on the failure energy.

3-2 Failure mode of DP/DP

Fig. (13a) shows a typical fracture surface of a spot weld which was failed in the interfacial failure mode at 8.5 KA. During interfacial mode spot weld is failed through the weld nugget centerline. As can be seen, interfacial failure mode is accompanied by little plastic deformation. Fig. (13b, c) shows a typical fracture surface of spot welds failed in the pullout failure mode(shear tearing and double pullout) at 9.5 KA and 10 KA receptively as shown in Table 2. The double pullout failure mode (DPF) fig (13c) is convert to pullout failure on expulsion as shown in table 2. Similar conclusion has been obtained on the effect of expulsion in galvanized low carbon steel [21]. In addition to the effect of expulsion on the static performance, Ma et al. [14], in their study on the failure behavior of DP600, reported that expulsion could decrease the fatigue limit of the spot weld.

Fig (13): Failure modes of DP600/DP600 RSW: (a): Interfacial Failure mode. (b): shear tearing. (c): double pullout failure .

Table 2: Effect of welding current on the fusion zone size and failure mode

Welding Current (KA)	Fusion Zone Size (mm)	Failure Mode
6.5	3.2	IF
7	4	IF
7.5	5	IF
8	5.8	IF
8.5	6.7	IF
9	8	PF+ shear tearing
9.5	8.5	PF+ shear tearing
10	8.75	DPF
11	9.2	DPF
12	6.25	PF

3-3 Microstructure of DP/DP

A typical macrostructure of DP600 RSW revealed three distinct zones, fusion zone (FZ), heat affected zone (HAZ) and base metal (BM) as shown in fig (14a). Fig. (14b) shows a typical micro-hardness profile of the DP600 steel, which exhibited a significant hardness increase from the base metal. The hardness of fusion zone is about 2.2 times more than that of the base metal, at a value of approximately 450HV. According to the temperature distribution, HAZ can be divided into two distinct metallurgical transformation zones, namely, high temperature HAZ (UCHAZ) above A_{C1}, middle temperature HAZ (ICHAZ) between A_{C1} and A_{C3}. optical microscope was used to examine the microstructural variations as shown in fig (15). Fig (15a) shows that the microstructure in the base metal basically consists of evenly distributed martensite(light brown) within the ferrite phase(white). The HAZ can be divided into two distinct regions: ICHAZ and UCHAZ. Fig. (15b) shows the boundary of ICHAZ and UCHAZ.

Fusion zone (FZ) microstructure Fig. (15c) predominately consists of full martensite phase which is responsible for the high value of measured hardness (450HV). Martensite formation in the FZ is attributed to the high cooling rate of RSW process due to the presence of water cooled copper electrodes and their quenching effect

as well as short welding cycle. For DP steels, the required critical cooling rate to achieve martensite phase in the microstructure can be estimated using the equation[20] **(**Log v = 7.42 – 3.13C – 0.71Mn – 0.37Ni – 0.34Cr – 0.45Mo), where V is the critical cooling rate in K h−1. For this steels the critical cooling rate is **407 (K s^{-1})(134C° s^{-1})**.

In RSW process, increasing sheet thickness reduces the cooling rate due to increasing the distance of liquid pool from the water cooled electrode with increasing sheet thickness. Gould et al. [22] developed a simple analytical model predicting cooling rates of resistance spot welds. According to this model, cooling rate for sheet having 1.5 mm thickness is about 4000 K s^{-1}[20]. These cooling rates are much higher than those needed to form martensite in the weld and HAZ in DP steels. Therefore, the high cooling rate during RSW, leads to the formation of martensite in the fusion zone of the DP600 steel.

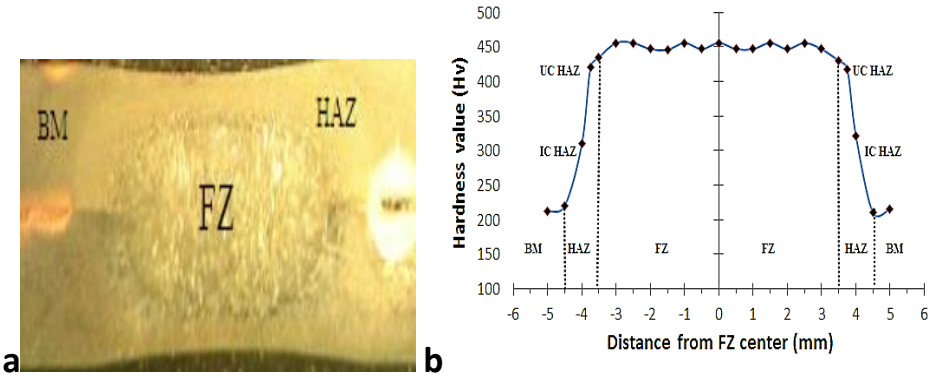

Fig (13): a: Macrograph of DP/DP and b: a typical micro-hardness profile of the DP600 steel after RSW.

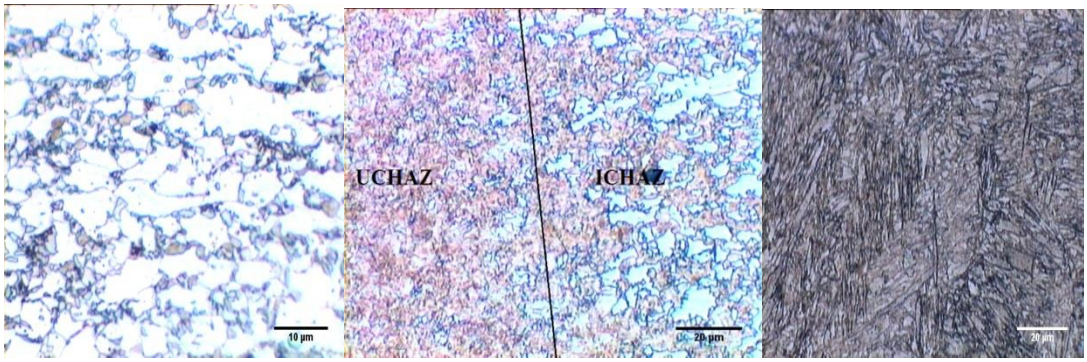

a b c

Fig (14): a: Base metal microstructure of DP600. b: ICHAZ- UCHAZ boundary. C: Fusion zone microstructure of DP600/DP600.

Table (3): summary showing materials, hardness characteristics and failure mode of dual phase steels, predicted critical fusion zone size and Experimental fusion zone size.

Material welding	t mm	H_{BM}	H_{MIN} ~ H_{FL}	H_{MAX} ~ H_{FZ}	H_{FL}/H_{FZ}	IF	PF	AWS $4t^{0.5}$	JIS, DVS $5t^{0.5}$	$\frac{4t}{pf}\left(\frac{HPFL}{HFZ}\right)$	(dcr) Experimental
DP600 / DP600	1.5	212	212	452	0.47	d ≤ 7 mm	d≥ 8 mm	4.9 mm	6.124 mm	5.62 mm	8 mm

*H: Hardness, MIN: Minimum, MAX: Maximum and FL: Failure Location

4-Conclusions

1- The conventional weld size guidance of $4t^{0.5}$ and $5t^{0.5}$is not sufficient to produce nugget pullout failure mode for DP600/ DP600 spot welds.

2 - Generally, increasing welding current increases the peak load and energy absorption primarily due to increasing the overall bond area caused by FZ size enlargement and as a consequence of the transition in failure mode from interfacial to pullout.

3 - Excessive welding heat input, where expulsion occurs, the peak load and energy absorption capability significantly reduce. Significant reduction of failure energy can be attributed to the reduction of weld fusion zone at high welding current.

4 - Welds with larger fusion zone size typically generate higher peak loads and energy absorption levels. Weld fusion zone size is the most critical factor in weld quality in terms of peak load and energy absorption for DP600/DP600.

References

1 – X. Sun, E. Stephens and M. Khaleel," Effects of Fusion Zone Size on Failure Modes and Performance of Advanced High Strength Steel Spot Welds ", SAE, PAPER SERIES 2006-01-0531.

2 - International Iron and Steel Institute, " ADVANCED HIGH STRENGTH STEEL (AHSS) APPLICATION GUIDELINES", Version 4.1, June 2009.

3 – F. Hayat, "Comparing Properties of Adhesive Bonding Resistance Spot Welding and Adhesive Weld Bonding of Coated and Uncoated DP 600 Steel ", JOURNAL OF IRON AND STEEI. RESEARCH, INTERNATIONAL. 18(9): PP. 70-78, (2011).

4 - J. Galán, L. Samek, P. Verleysen, K. Verbeken and Y. Houbaert, "Advanced high strength steels for automotive industry(·) " rEviSTa DE METalUrGia, 48 (2), MarZo-aBril, PP. 118-131, 2012.

5 - M. MARYA and X. Q. GAYDEN "Development of Requirements for Resistance Spot Welding Dual-Phase (DP600) Steels Part 1 — The Causes of Interfacial Fracture " WELDING JOURNAL, pp. 173-182, NOVEMBER 2005.

6 – Z. Xiaoyun, C. Guanlong, Z. Yansong, L. Xinmin, "Improvement of resistance spot weldability for dual-phase (DP600) steels using servo gun", journal of materials processing technology 2 0 9, PP. 2671–2675, 2 0 0 9.

7 - TUMULURU, "Resistance Spot Welding of Coated High-Strength Dual-Phase Steels ", WELDING JOURNAL, PP. 31-37, AUGUST 2006.

8 - R. KUZIAK, R. KAWALLA, S. WAENGLER, "Advanced high strength steels for automotive industry " ARCHIVES OF CIVIL AND MECHANICAL ENGINEERING, Vol. VIII, No. 2, pp103-117, 2008.

9 - H. Hofmann, D. Mattissen, T. W. Schaumann, "Advanced cold rolled steels for automotive applications", Mat.-wiss. u. Werkstofftech, 37, No. 9, PP. 716-723, 2006.

10 - F. Hayat & İ. Sevim "The effect of welding parameters on fracture toughness of resistance spot-welded galvanized DP600 automotive steel sheets" Int J Adv Manuf Technol 58, PP.1043–1050, 2012 .

11 - S.B. Behravesh, L. Liu, H. Jahed, S. Lambert, G. Glinka and Y. Zhou, "Effect of Nugget Size on Tensile and Fatigue Strength of Spot Welded AZ31 Magnesium Alloy", SAE International SAE, PAPER SERIES 2010-01-0411.

12 - ANSI/AWS/SAE, " Test Method For Evaluating The Resistance Spot Welding Behavior of Automotive Sheet Steel Materials", American Welding Society, 2012.

13 - H. Zhang and J. Senkara: "Resistance Welding: Fundamentals and Applications", (CRC Group, Boca Raton, FL, 2006).

14 - C. Ma, D.L. Chen, S.D. Bhole, G. Boudreau , A. Lee , E. Biro "Microstructure and fracture characteristics of spot-welded DP600 steel " Materials Science and Engineering A 485, PP. 334–346, (2008) .

15 - Gilvan Prada, "Correlation Study of Spot Welded Specimens'Behavior using Finite Element Method", SAE, PAPER SERIES 2008-36-0100.

16 - M. Pouranvaria, S.P.H. Marashi, "Failure mode transition in AHSS resistance spot welds. Part I. Controlling factors ", Materials Science and Engineering A 528, PP. 8337– 8343, (2011).

17- M. Goodarzia, S.P.H. Marashib, M. Pouranvari, "Dependence of overload performance on weld attributes for resistance spot welded galvanized low carbon steel", Journal of Materials Processing Technology, 209, PP. 4379–4384, (2009). .

18 - Industrial Standards Committee, Tokyo, ‘Method of inspection for spot welds’, JIS Z 3140, Japanese Japan, (1989).

19 - ‘Resistance spot welding’, DVS 2923, German Standard. Du¨ sseldorf , Germany, 1986.

20 - M. Pouranvari, S.P.H. Marashi, D.S. Safanama, "Failure mode transition in AHSS resistance spot welds. Part II: Experimental investigation and model validation ", Materials Science and Engineering A 528, PP. 8344– 8352, (2011).

21 - M. Pouranvari, S.P.H. Marashi, "On the failure of low carbon steel resistance spot welds in quasi-static tensile–shear loading ", Materials and Design 31, 3647–3652, (2010) .

22 - E. GOULD, S. P. KHURANA, T. LI, "Predictions of Microstructures when Welding Automotive Advanced High-Strength Steels ", WELDING JOURNAL, MAY 2006, pp111s-116s.